ORIGINAL PAPER

Chitosan hydrogels chemically crosslinked with L-glutamic acid and their potential use in drug delivery

D. E. Rodríguez-Félix[1] · D. Pérez-Caballero[1] · T. del Castillo-Castro[1] ·
M. M. Castillo-Ortega[1] · Y. Garmendía-Diago[1] · J. Alvarado-Ibarra[1] ·
M. Plascencia-Jatomea[2] · A. S. Ledezma-Pérez[3] · S. E. Burruel-Ibarra[1]

Abstract

Controlled drug release systems have the characteristics of eliminating or reducing side effects and producing a therapeutic concentration of the drug that is stable in the body. The synthesis of hydrogels from natural polymers allows innovation in new materials that promote more effective, selective and safe therapies, in comparison with hydrogel systems based on synthetic polymers where their main limitation may be their biocompatibility and degradation. For this reason, in this work the synthesis of hydrogels of chitosan crosslinked with glutamic acid is proposed as the basis of new trends in smart materials for their potential use in the controlled release of drugs, the hydrogels were prepared from an amidation reaction between the amino groups of chitosan and the carboxyl groups of L-glutamic acid, using *N*-(3-Dimethylaminopropyl)-*N'*-ethylcarbodiimide hydrochloride (EDC) as activator of the carboxyl groups. The hydrogels obtained were characterized by SEM, FTIR, TGA techniques, swelling kinetics and antimicrobial activity. They exhibited excellent swelling capacity and good performance when exposed to different pH and temperature conditions. The bacterial inhibition percentages demonstrated the antimicrobial activity of chitosan hydrogels and the results obtained potentially favored their use as reservoirs for controlled drug release.

Keywords Hydrogels · Chitosan · L-Glutamic acid crosslinker · Amidation reaction · Swelling kinetics · Controlled release

✉ D. Pérez-Caballero
danay.perezcaballero@gmail.com

[1] Departamento de Investigación en Polímeros y Materiales, Universidad de Sonora, 83000 Hermosillo, Sonora, Mexico

[2] Departamento de Investigación y Posgrado en Alimentos, Universidad de Sonora, 83000 Hermosillo, Sonora, Mexico

[3] Centro de Investigación en Química Aplicada, Saltillo, Coahuila, Mexico

Introduction

Currently, natural polymers are intended to replace synthetic materials commonly used in biomedical and pharmaceutical applications due to their biodegradability and biocompatibility. Its various properties allow innovating in new materials that promote more effective, selective and safe therapies. One of the most stable and used systems for this purpose is hydrogels [1]. Hydrogels are crosslinked polymeric materials in the form of a three-dimensional network obtained using natural polymers or synthetic monomers. Hydrogels have the capacity to absorb large amounts of water, swell and increase their volume considerably without losing their shape until they reach their maximum swelling degree [1–4]. The factors that determine the swelling degree are the hydrophilicity of the polymer chains, given by the presence of hydroxyl (–OH), carboxyl (–COOH), amides (–CONH$_2$) and sulfonyl (–SO$_3$H) groups, along the polymer chains [3, 5, 6]. Among the most widely used natural polymers for the preparation of hydrogels is chitosan, which is known for its excellent properties. It is a long-chain linear polysaccharide formed by *N*-glucosamide and *N*-acetyl glucosamide units linked by *β* (1–4) bonds and is obtained by alkaline deacetylation of chitin at high temperatures; during this process, the acetyl groups are partially removed from chitin, leaving the amino groups (–NH$_2$) characteristic of chitosan [7–12]. The presence of the amino groups in the structure of chitosan makes it one of the most versatile materials studied, since it offers the possibility of carrying out a wide variety of modifications, such as enzymatic anchoring reactions, grafting reactions, crosslinking reactions, obtaining of suitable materials with properties to be applied in biotechnology, biomedicine, pharmaceuticals, textiles, food, water treatment and agriculture [2, 11, 13–19]. The biological properties of chitosan have given it an important connotation in the study of new materials for formulation and administration of new pharmaceutical forms [20]. Some of the functional properties of chitosan are: biodegradability, biocompatibility, biological activity, self-adhesion, filmogenic capacity, hemostatic capacity, absorption promoter, antimicrobial and antioxidant [11, 19, 21–23]. It has also been detected that it does not have an acute cytotoxic effect [24]. Although there are documented studies of the use of chitosan hydrogels with poly(gamma-glutamic acid) for biomedical applications [1, 4, 25–29], there are few investigations where chitosan hydrogels are synthesized using the acid glutamic as a crosslinking agent. Glutamic acid is an amino acid that is synthesized in the human body from arginine and proline. In the body, it is converted to glutamine, it is the only amino acid metabolized by the brain in addition to being a precursor agent for collagen, an essential protein for tissue regeneration. It has two carboxylate groups in its structure, which allows it to bind to the amine group of chitosan, reinforcing its hydrophilic properties and giving significant stability to the structure of hydrogels when used as a crosslinking agent [1, 30–36]. Singh et al. synthesized hydrogels of chitosan and soluble glutamic acid in a wide pH range, through a treatment with supercritical CO$_2$ [32]. Tsao et al. improved the physical properties and biocompatibility of chitosan hydrogels using glutamic acid as solubilizing and crosslinking agents simultaneously [37].

Thangavel et al. synthesized hydrogels of chitosan and glutamic acid by physical crosslinking that increased collagen deposition, vascularization, and tissue regeneration in diabetic wounds [36]. The design and application of controlled drug delivery systems is currently one of the most relevant aspects in the development of new dosage forms. The use of polymeric materials as drug carriers to regulate and dose their release in specific applications is a perspective that has generated great interest today. Polymeric materials used for drug delivery can improve pharmacokinetics, therapeutic index, decrease adverse reactions and improve the efficiency of the drug delivery system [22, 38–42]. Within these release systems it is important to study neomycin sulfate, which is a broad-spectrum aminoglycoside antibiotic widely used to prevent or treat skin infections caused by bacteria [43, 44]. In order to develop hydrogels based on natural polymeric materials to be used as controlled drug delivery systems, in our study we report the design of glutamic acid cross-linked chitosan hydrogels with good physicochemical properties, swelling capacity and antimicrobial activity for its subsequent application in the release of neomycin sulfate as a model drug. This synthesis method allows the chemical crosslinking of chitosan, without the presence of heat, obtaining an irreversible crosslinking characteristic of chemical hydrogels, which favors that the polymeric matrix presents greater stability in comparison with the physical crosslinking reported in the literature for this type of hydrogels [32, 36, 37].

Experimental

Materials

Chitosan of medium molecular weight (molecular weight of 190–310 kDa), 75–85% deacetylation, L-glutamic acid with 99.5% purity and *N*-(3-Dimethylaminopropyl)-*N′*-ethylcarbodiimide hydrochloride (EDC) with 99% purity, Neomycin sulfate model drug were supplied by Sigma-Aldrich. Ethyl ethanol 99.91% used for washes was supplied by Faga Lab. *Escherichia coli* (*ATCC*25922), *Staphylococcus aureus* (*ATCC*6538), *Pseudomonas aeruginosa* (*ATCC*9027), *Salmonella typhimurium* (*ATCC*14028), *Bacillus subtilis* (*ATCC*6633) and *Candida albicans* (*ATCC*10231) provided by DIPA microbiology laboratory of the University of Sonora were used as bacteria models to evaluate the antimicrobial activity of hydrogels.

Synthesis of chitosan hydrogels

Chitosan hydrogels were synthesized using diluted acetic acid as solvent, glutamic acid as crosslinking agent and EDC as catalyst; cross-linking was carried out by an amidation reaction between the amino groups of the chitosan and the carboxyl groups of glutamic acid (Fig. 1). To obtain the hydrogels, chitosan sponges were first prepared; for which, 0.5 g of chitosan were dissolved in 10 ml of acetic acid 1 % (v/v) using magnetic stirring for 30 min. The solutions obtained were passed to the molds and frozen for 24 h. Then they were dried by lyophilization. Subsequently, the

Table 1 Quantities used for the preparation of hydrogels

Hydrogel	Chitosan (g)	L-glutamic acid (g)	EDC (g)
HG$_1$	0.5	0.0375	0.15
HG$_2$	0.5	0.0250	0.10
HG$_3$	0.5	0.0125	0.05

Table 2 Washing proportions

Num. of washes	% Ethanol	% Water
1	100	0
2	70	30
3	50	50
4	0	100

dried sponges were immersed in 10 ml of aqueous solution of glutamic acid with different concentrations 0.375, 0.25 and 0.125 % (w/v), then 0.15, 0.1 and 0.05 g of EDC were added, respectively, allowed to stand for 24 h (Table 1). Subsequently, a series of washes were carried out in ethanol/water mixtures and finally in water (Table 2); then they were frozen and dried using a Labconco Freezone 4.5 freeze dryer.

Characterization

Scanning electronic microscopy (SEM)

The morphology of the hydrogels was studied by SEM. Samples were obtained by carefully cutting the surface of the dry hydrogel with a brittle cutter, then coated with gold-palladium to impart conductive properties, and viewed on a Jeol JSM 6410LV brand scanning electron microscope.

From the obtained micrographs, the pore size was determined using the ImageJ software. The diameters of each pore were measured. The reported pore size is an average of all the measurements taken.

The effect of the crosslinking agent concentration in each sample was evaluated from the pore size measurements.

Fourier transform infrared spectroscopy (FTIR)

A characterization of the hydrogels obtained by the FTIR technique was performed using the Perkin Elmer Frontrier equipment in a KBr pellets, a spectrum scan was carried out from 4000 to 500 cm^{-1}. This study was done in order to determine if carried out the crosslinking reaction between the amine group of chitosan and the carboxyl group of L-glutamic acid from an amidation reaction.

Swelling kinetics study

Dry hydrogel samples with dimensions 10 mm in diameter and 1.5 mm in thickness were cut. They were immersed in vessels with 30 ml of water at room temperature and the weight of the hydrogels was monitored at 10 min time intervals. The hydrogels were weighed using an analytical balance and previously dried with filter paper to remove water accumulated on the surface of the sample. The study was carried out by triplicate. The swelling ratio was calculated using Eq. 1.

$$\delta = \frac{W_s - W_d}{W_d} \tag{1}$$

where W_s is the weight of the swollen gel at different times and W_d is the weight of the dry gel.

Using the same procedure, substituting the water for a buffer solution at pH 3 and pH 7.4, with temperatures of 25 °C and 37 °C, the effect of temperature and pH on the swelling of the hydrogel was determined.

The solvent transport mechanisms were also determined in both systems (deionized water and in the buffer solution). According to what is stated in Fick's second law, the power law can be used to analyze the type of diffusion of a solvent into the hydrogel. (Eq. 2).

$$F = k * tn \tag{2}$$

where F is expressed as a fraction related to the amount of water accumulated by the hydrogel, k is the constant related to the network system and the swelling medium and n is the diffusion exponent, which governs the mode of transport of the water. Generally this equation applies in the initial stages of swelling, that is, up to almost a 60 % increase in the mass of the hydrogel. Several definitions for F have been reported, including the one defined by Karadag et al. (Eq. 3) [45].

$$F_k = (W_t - W_0)/W_0 \tag{3}$$

To determine the diffusion mechanisms, the ln is applied taking into account the data up to 60% of the increase in the weight of the hydrogel. The results of ln$F$ are plotted against ln$t$, from the values of swelling obtained as the definition of Karadag et al. The values of the diffusion coefficient (n) were determined and the mechanisms from which the absorption of the solvent in the hydrogel occurs were analyzed using Table 3.

Thermogravimetric analysis (TGA)

A TGA was performed to sample, under a nitrogen controlled atmosphere as a function of temperature, while the latter increases with constant rate 10 °C/min. The study was carried out using a Perkin Elmer 1 TGA device, in a temperature range of 25–800 °C that allows us to know the thermal stability of the chitosan hydrogel in comparison to the stability of each individual material (chitosan, glutamic acid).

Table 3 Classification of transport mechanisms

Transport mechanisms	Diffusion coefficient [n]	Process speed
Lower Fickian diffusion	$n < 0.5$	$v_{\text{diffusion}} \ll v_{\text{relaxation}}$
Inferior Fickian diffusion (case I)	$n = 0.5$	$v_{\text{diffusion}} \ll v_{\text{relaxation}}$
Anomalous or non-Fickian diffusion	$0.5 < n < 1$	$v_{\text{diffusion}} \approx v_{\text{relaxation}}$
Non-Fickian diffusion (case II)	$n = 1$	$v_{\text{diffusion}} \gg v_{\text{relaxation}}$

The equipment's software was used to obtain the temperatures and graphically represent the TG curves of the thermograms.

Antimicrobial activity evaluation

A cell viability analysis was performed to determine the antimicrobial activity of the chitosan hydrogels, starting from 6 species of bacteria (*E.coli, S. aureos, Pseudomonas, Salmonella, B. subtilis and Candida*), by the technique of reduction of Resazurin.

Firstly, 100 ml of previously prepared nutrient broth medium were dispensed into 12 10 ml glass tubes. They were sterilized for 21 min at 121 °C and subsequently allowed to cool. These tubes with the nutrient broth were then inoculated with the bacteria and incubated for 24 h at 37 °C. Dry hydrogels were cut into 0.5 cm diameter cylinders, sterilized for 5 min with UV light, and placed on a 6-well sterile plate. Then, the hydrogels were inoculated with 500 µl of inoculum of each bacteria with a known concentration of 1×10^8 CFU/ml adjusted to the McFarland standard and were incubated for 24 h at 37 °C. After 24 h, the inoculated hydrogels were resuspended in 5 ml of sterile PBS 1x solution and were shaken 25 times for 1 min. In the same way, 500 µl of bacterial inoculum were resuspended in 5 ml of PBS 1x solution and were shaken 25 times for 1 min. Then, 100 µl aliquots were taken from both each hydrogels-inoculum suspension and bacterial-inoculum suspension and were placed in 96-well microplates by triplicate. The $OD_{570\,\text{nm}}$ (time 0) was read in a plate reader from Elisa. The microplates were incubated at 37 °C for 24 h and the $OD_{570\,\text{nm}}$ was read again. Subsequently, 5 µl of the 0.02 % Resazurin reagent were added per well. The microplates were incubated approximately 4 h at 37 °C, after this time the $OD_{570\,\text{nm}}$ was read again. The percentage viability of the bacteria was determined with respect to the control of normal growth.

Drug release

The chitosan hydrogels cut with dimensions 10 mm in diameter and 1.5 mm in thickness, were loaded with 1 ml of neomycin sulfate from a 20 mg/ml stock solution, for 24 h. Once the samples were loaded, they were frozen and subsequently lyophilized. Drug release was carried out at 25 °C with constant stirring, in 50 ml of buffer solution at pH 4.6 for 5 h. The neomycin sulfate-loaded hydrogels were immersed in the buffer solution and the 3 ml solution was aliquoted at 30 min intervals and returned

to the medium to maintain a constant volume. The amount of drug released was determined by measurements on an Agilent UV–Vis spectrophotometer at $OD_{300\,nm}$.

Mathematical modelling

To determine the kinetic parameters and the predominant drug release mechanism in chitosan hydrogels, 3 mathematical models were studied, the results obtained were compared between them using Origin 8.5 and Excel 10 as statistical platforms.

Korsmeyer–Peppas model

The mathematical model of Korsmeyer–Peppas, exponentially relates the release of the drug with the elapsed time. This model is mainly adjusted to 60 % of the amount of drug released and is used to determine if the release kinetics follows a diffusion mechanism that obeys Fick's first law [46]. The general form of this model is as follows:

$$\frac{M_t}{M_\infty} = kt^n \tag{4}$$

where t is the release time, M_t is the amount of drug released at time t, M_∞ is the amount of drug released at equilibrium, k is a kinetic constant that depends on the structural characteristics of the polymeric matrix and n is the exponent diffusional, which is an indicator of the drug release mechanism. The exponent can take values close to 0.5, which indicates that the release follows a Fickian behavior, with diffusion being the main mechanism involved. Values of 0.5–1.0 for anomalous or first order transport, where the release occurs by diffusion and relaxation of the polymeric chains and values equal to 1 for the transport called type II (order 0) that indicate that the release is controlled by processes of relaxation of the polymer, which implies a constant release as a function of time [46].

Higuchi model

A linear relationship is obtained between the amount of drug released and the square root of the time when the release follows a simple Fickian diffusion, then the results are adjusted to the Higuchi model [47, 48]. The general equation of this model is the following:

$$\frac{M_t}{M_\infty} = kt^{0.5} \tag{5}$$

where t is the release time, M_t is the amount of drug released at time t, $M\infty$ the amount of drug released at equilibrium, and k is known as the Higuchi release constant. This model assumes $n = 0.5$ in the equation.

Zero-order model

When the same amount of drug is released per unit of time during the release process, the predominant mechanism is zero order, it is the ideal pattern that the

release of a drug should follow, if the goal is to achieve constant and prolonged activity, where *n* is equal to 1 [49]. It is expressed as follows:

$$\frac{M_t}{M_\infty} = kt \tag{6}$$

Results and discussion

Synthesis of chitosan hydrogels

Chitosan hydrogels chemically crosslinked with glutamic acid and EDC as catalyst were obtained. This synthesis method was selected because it allowed us to obtain chitosan hydrogels with desired characteristics. In this way transparent hydrogels; with a light-yellow color, characteristic of chitosan and well-defined shape, were obtained. On the other hand, the increase in the proportion of the crosslinking agent increased the consistency of the hydrogels, improving their handling. The amidation reaction that occurs between the amino groups of chitosan and the carboxyl groups of glutamic acid resulting in the crosslinking of chitosan, is shown in Fig. 1. The physicochemical and swelling properties of the synthesized hydrogels are shown below.

Scanning electronic microscopy (SEM)

The hydrogels obtained were analyzed by means of scanning electron microscopy (Fig. 2), to determine the morphology and porosity of the surface of the hydrogels.
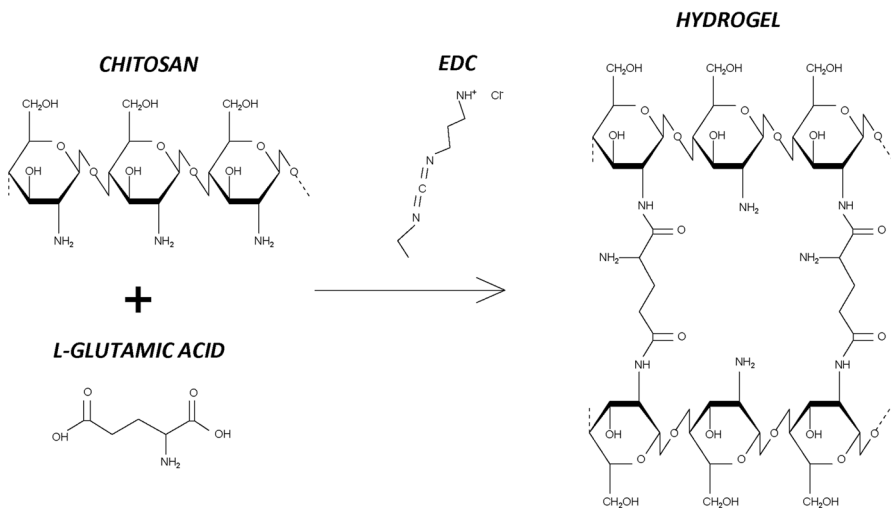

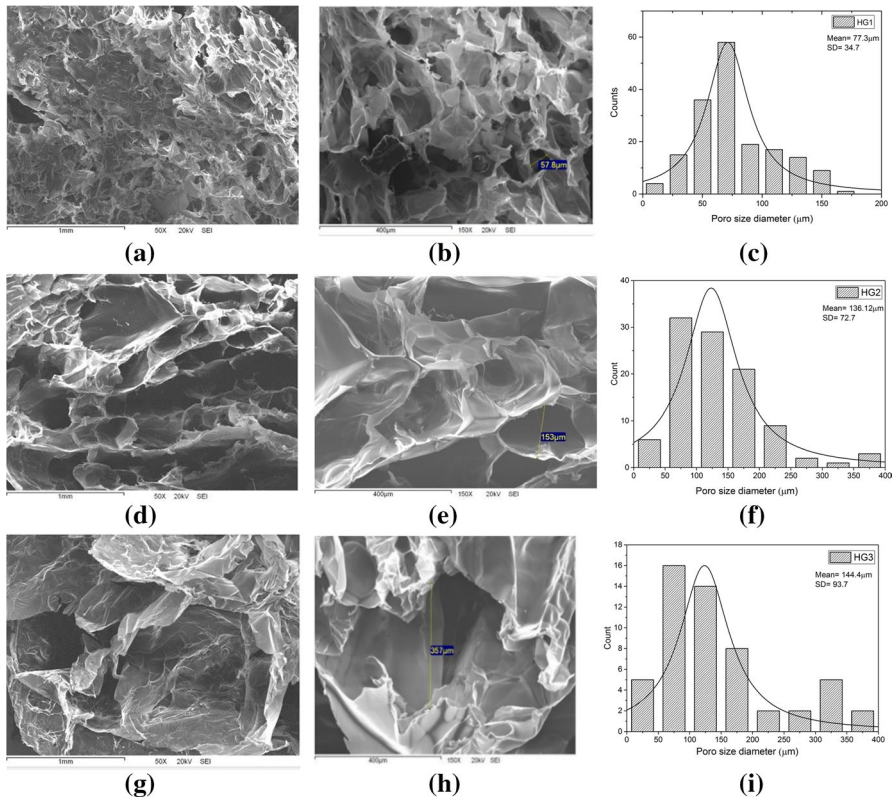**Fig. 1** Chitosan crosslinking reaction

Fig. 2 SEM: **a**, **b** and **c** HG1; **d**, **e** and **f** HG2; **g**, **h** and **i** HG3; corresponding to 50 increases,150 increases and size porous distribution, respectively

SEM images show that the hydrogels studied have a similar appearance in terms of surface morphology, but a difference in the distribution and size of the pores was observed. On this manner, as the amount of crosslinking agent increases, the hydrogel structure becomes more compact and homogeneous, so the distribution becomes more uniform, and the pore size decreases, corresponding to what observed for each hydrogel.

$$\text{HG1 } ps < \text{HG2 } ps < \text{HG3 } ps$$

where *ps* is pore size.

Fourier transform infrared spectroscopy (FTIR)

Figure 3a represents the FTIR spectra of chitosan and glutamic acid. The characteristic signs of chitosan were observed: a band at 3441 cm^{-1}, assigned to stretching vibration of hydroxil group (O–H) and amino group (N–H); a band at 2894 cm^{-1}, assigned to stretching vibration (C–H) of the methylene group (–CH_2) [50, 51];
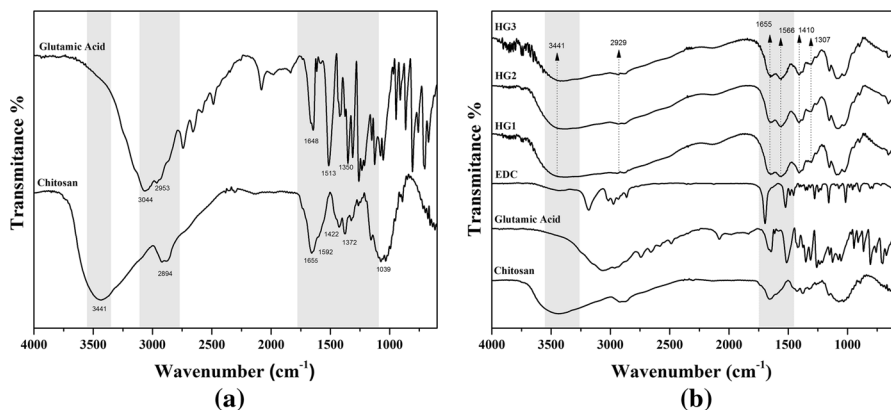
Fig. 3 FTIR spectra. **a** Chitosan and glutamic acid, **b** Synthesized Hydrogels HG1, HG2, HG3 and of the materials used for the synthesis

the stretch of amide I (C=O) at 1658 cm^{-1} and the peak corresponding to amide II at 1592 cm^{-1}, the signal at 1422 cm^{-1} is assigned to the bending vibration of the (N–H) amino group; at 1372 cm^{-1} it is assigned to the flexing vibration of the O-H hydroxyl [10, 32, 52]. The characteristic peaks of glutamic acid are shown, in the range of 3000 to 3500 cm^{-1} a signal is assigned to the OH stretch, which overlaps the stretching of the primary amino group, both symmetric and asymmetric. The signal is shown at 1648 cm^{-1} corresponding to the stretching of the carbonyl group (C=O) and 1513 cm^{-1} stretching of the amino group (N–H) [36, 37]. A comparative graph of the hydrogels obtained is shown in Fig. 3b. A characteristic band appears at 3441 cm^{-1} corresponding to the stretching vibration of the hydroxyl group and the stretching vibration of the amino group (N–H) corresponding to a primary amine NH$_2$. The stretching of amide I at 1655 cm^{-1} (stretching of the carbonyl group, the peak corresponding to(N–H)bending vibration of amide II at 1566 cm^{-1}, the signal at 1410 cm^{-1} is assigned to the vibrational flexion of (C–H) bonds and a signal corresponding to the (N–H) deformation between 1307 cm^{-1} assigned to an amide III [32, 35, 37, 53]. The increases in the bands (N–H) (amide I and II) of the hydrogels with respect to chitosan were marked, these results indicate that the amidation reaction occurred favorably, since once the hydrogel was formed, the proportion of Amide bonds should increase with respect to those existing in the polymer chains. The intensity of the amide II signal increases in hydrogels as a result of chemical crosslinking of the hydrogel [53].

Swelling kinetics

Figure 4 shows the behavior of the swelling ratio of the hydrogels at different studied times intervals. A rapid absorption of water is shown in the first few minutes, which can occur due to the presence of the hydrophilic groups present in the chitosan, followed by a gradual increase in absorption until it reaches its swelling equilibrium. Sample HG1 reached its equilibrium swelling at 100 min and sample HG2

Fig. 4 Swelling kinetics of hydrogels in deionized water
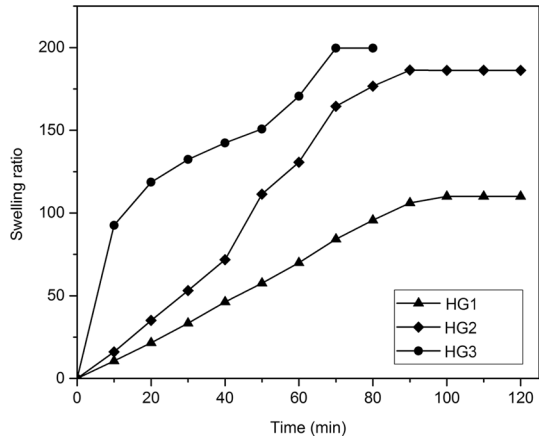
at 90 min. These hydrogels have a slower water absorption capacity because their structure is more compact and the pore sizes are smaller. The HG3 sample reached its maximum swelling at minute 70 which is attributed to having a larger pore size due to a lower proportion of crosslinking agent, making it easier for water to penetrate and reach equilibrium faster. The factors that determine the degree of swelling are the hydrophilicity of the polymer chains and the crosslinking density.

Figure 5a, b show that hydrogels swollen in the buffer solution at pH 3 have a higher swelling ratio than hydrogels swollen at pH 7.4 for both temperatures (25 °C, 37 °C), which is mainly attributed to the chemical characteristics of the chitosan. Taking into account that the pka of the amino group of chitosan and glutamic acid is 6.5 and 9.67, respectively, when the hydrogel is exposed to pH 3 below its pka, the amino groups present in the polymer structure are protonated NH_3^+, the electrostatic repulsion forces between the chains increase, the interactions by hydrogen bonds are weakened and, therefore, its capacity swelling
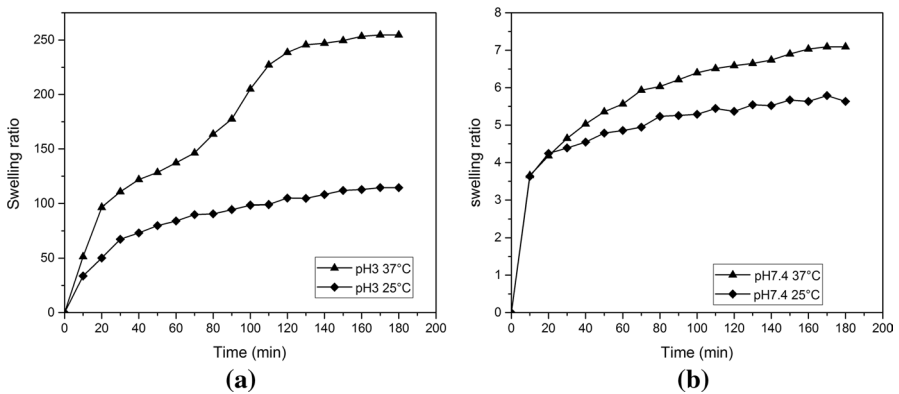

Fig. 5 Swelling kinetics of chitosan hydrogels in buffer at **a** pH 3 and **b** pH 7.4 for sample HG1

increases. At pH 7.4 there was little or no protonation of amino groups the swelling ratios were lower [4, 54]. Furthermore, interesting behavior in the swelling kinetics is observed with increasing temperature, attributed to relaxation of polymer chains, causing the dissociation of the hydrogen bonds present in the structure and allowing the entry of greater volumes of water into the hydrogel.

Thangavel et al. report the value of the swelling ratio for glutamic acid crosslinked chitosan hydrogels in PBS pH 7.4 at 37 °C between 1 and 1.5 [36]. If we compare it with the results obtained in our study under the same conditions, a swelling ratio between 5.7 and 7 was shown. The hydrogels obtained by chemical synthesis may be more stable due to the covalent bonds formed by the crosslinking of the polymer chains, the which are irreversible, allowing the hydrogels to be exposed to different environmental conditions such as pH and temperature, without their breakdown occurring.

The data of the swelling kinetics were adjusted to the transport mechanisms represented in Table 3. The curves were linearized at the beginning of the swelling, until an increase in the mass of the hydrogel to 60 %, observing an excellent linear correlation. The swelling of the system is determined according to the diffusion rates of the water with respect to the relaxation rate of the polymeric matrix. Table 4 summarizes the data obtained that determine the mechanism of water penetration in the hydrogel. HG3 hydrogel is observed to have a higher swelling rate relative to HG1 and HG2 hydrogels in deionized water. In the case of hydrogels HG1 and HG2, the transport corresponds to case II of non-Fickian diffusion, so that the penetration of water in the hydrogel is controlled by the relaxation rate of the polymeric chains. In the case of HG3, the rate of penetration of the water is much lower than the rate of relaxation of the chains, for HG1 swollen at different pH and T values, it is observed that the n approaches 0.5, so it follows a Fickian diffusion behavior where the swelling process is controlled only by the phenomenon of water diffusion through the polymeric matrix.

Table 4 Classification of transport mechanisms

Swelling condition	Diffusion coefficient [n]	$k[\min^{-n}]$	R	R^2	Transport mechanisms
Deionized water HG1	1	0.9202	0.9999	0.9999	Non-Fickian diffusion case II
Deionized water HG2	1	1	0.9968	0.9923	Non-Fickian diffusion case II
Deionized water HG3	0.3	46.9268	0.9964	0.9903	Lower Fickian diffusion
G1 37°C pH 3	0.3	36.6341	0.9985	0.9962	Lower Fickian diffusion
HG1 25°C pH 3	0.3	24.3787	0.9972	0.9941	Lower Fickian diffusion
HG1 25°C pH 7.4	0.2	2.5366	0.9866	0.9619	Lower Fickian diffusion
HG1 37°C pH 7.4	0.2	0.2504	0.9979	0.9954	Lower Fickian diffusion

Thermogravimetric analysis (TGA)

Thermogravimetric analysis, the weight loss of the material is shown as a function of temperature. Figure 6 shows the TG and DTG curves for glutamic acid, chitosan, and chitosan hydrogels.

The glutamic acid thermogram shows a decomposition in three stages, one peak at a degradation Tmax at 216 °C with a weight loss of 10 %, another peak at 261 °C with a weight loss 29% and a third stage where a weight loss of 48 % is observed, corresponding to 580 °C. The chitosan thermogram shows a degradation in three stages: at 50 °C, 4 % attributed to water loss due to the characteristic hydrophilicity of chitosan [55], at 300–350 °C interval, 27 % weight loss, caused by the depolymerization of the polymer chains [10, 55] and at 614 °C 59 % weight loss, related to the decomposition of the pyranose ring present in the structure [51, 56]. At 680 °C a full degradation was observed. The chitosan hydrogel showed a degradation in three stages at Tmax of 49, 268 and 800 °C, with weight losses of 5, 36 and 59 %, respectively. The first stage is related to moisture loss, and the second and third stages are related to material degradation. As can be seen in the second stage of degradation, the hydrogel presents a lower thermal stability compared to chitosan and this behavior is attributed to the presence of the crosslinker.
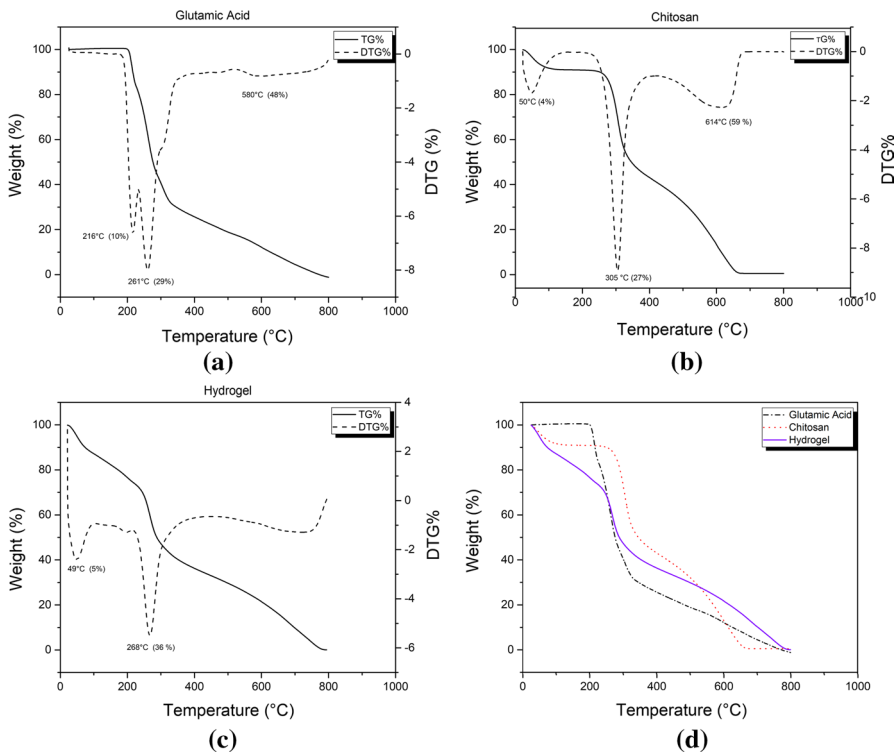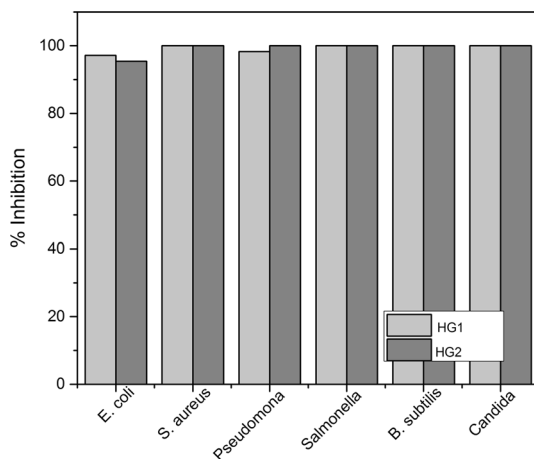

Fig. 6 TGA Thermograms: **a** L-Glutamic Acid, **b** Chitosan, **c** Hydrogels and **d** TG

Table 5 Bacterial inhibition of hydrogels on the studied species

Bacterias	HG1 (%)	HG2 (%)
E. coli	97.14 ± 0.1	95.45 ± 0.02
S. aureus	100	100
Pseudomonas	98.3 ± 0.01	100
Salmonelas	100	100
B. subtilis	100	100
Candida	100	100

Fig. 7 Effect of hydrogels on the viability of the studied species

Antimicrobial activity evaluation

The antimicrobial activity of the hydrogels was evaluated using the resazurin reduction technique [57]. Table 5 and Fig. 7 the percentage of bacterial inhibition is observed for the evaluation times 4 h of incubation and then at 24 h. Both hydrogels (HG1, HG2) had the same behavior, exhibiting significant antibacterial activity and a high percentage of growth inhibition for each species. The results show that chitosan-glutamic acid hydrogels have a bacteriostatic effect, the levels of bacterial inhibition favor the possible application of these materials in the drugs' controlled release. The inhibitory effects of hydrogels are attributed to the presence of the amino group in the structure of the chitosan. The NH_2 in the form of the NH_3^+ ion binds to the anions present in the outer wall of the cell and inhibits cell permeability, causing cell lysis [58]. It also has antifungal properties related to the affectation of the integrity of the fungal plasma membrane that causes an osmotic imbalance and the inhibition of the growth of the microorganism [59, 60].

Drug release

In all the cases studied, between 70 and 85% of the drug was released as shown in Fig. 8. In the case of hydrogels (HG1) with a higher concentration of crosslinker and smaller pores, a more controlled release over time is observed, showing 71% release of the drug, unlike the HG3 hydrogel, which has a lower concentration of glutamic acid, higher degree of swelling and larger pore size, allowing easy diffusion of the drug in the diffusion mean. The HG2 hydrogel exhibited 77% drug release. When comparing the three samples HG1, HG2, HG3 in terms of the concentration of crosslinker and the swelling kinetics presented during the characterization, a behavior of entry and exit of the fluid to the matrix is observed that is due to the pore size, swelling and flexibility of the chains.

Mathematical model

From the experimental results, we proceeded to determine which of the mathematical models described above is the one that provides the best fit. This was determined from statistical criteria, such as the correlation coefficient R^2 and the adjusted correlation coefficient R^2_{adj}. To evaluate the fit of release models with the same number of parameters, the correlation coefficient can be used. However, when evaluating models of different quantities of parameters, it is advisable to use the adjusted correlation coefficient [61]. In all cases, values below 60 % of the release were taken and OriginPro analysis software was used.

Table 6 shows that for the three hydrogels, the Korsmeyers–Peppas and Higuchi models show a higher adjusted correlation coefficient, but not zero-order model.

By fitting the drug release data to the Korsmeyer–Peppas model, n values between 0.5 and 1 are obtained for the three hydrogels (HG1, HG2, HG3), which means that an anomalous type mechanism regulates the release of neomycin sulfate. In this type of mechanism, the processes of diffusion and relaxation of the polymer matrix chains predominate. The Higuchi model predicts the behavior of the release rate through the

Fig. 8 Neomycin Sulfate release profiles in % performed at pH 4.6 and 37 °C
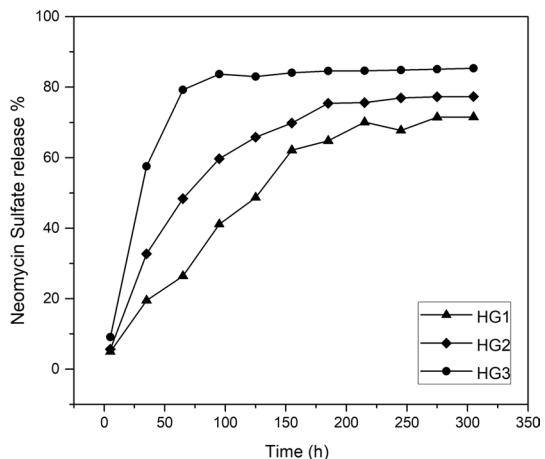
Table 6 Classification of transport mechanisms

Hydrogel	Korsmeyer–Peppas				Higuchi			0 Order		
	n	k	R^2	R^2_{adj}	k	R^2	R^2_{adj}	k	R^2	R^2_{adj}
HG1	0.7187	0.0212	0.9928	0.9910	0.0697	0.9357	0.9196	0.0014	0.8138	0.7673
HG2	0.8166	0.0205	0.9927	0.9890	0.0813	0.9982	0.9973	0.0020	0.8692	0.8038
HG3	0.8684	0.0272	0.9909	0.9817	0.1191	0.9995	0.9989	0.0011	0.9181	0.8362

Higuchi rate constant, as shown in Table 6, the hydrogel with the lowest concentration of crosslinking agent presented the highest release rate. This phenomenon may be due to the morphology of the hydrogels in terms of pore size, which is related to the results obtained in the swelling kinetics for the three hydrogels where HG1 presented a lower swelling kinetics than that obtained for the HG2 hydrogels and HG3, since HG1 has a smaller pore size, its chains are more compact because the amount of crosslinking agent used in the synthesis is greater with respect to HG2 and HG3.

Conclusions

Chitosan hydrogels were synthesized from an amidation reaction, using simple, ecological and low cost crosslinking methods. FTIR spectra confirmed the crosslinking reaction between the chitosan amine and the carboxyl group of glutamic acid. SEM measurements revealed scattered structures and more defined pore sizes for hydrogels with higher glutamic acid concentration. The swelling kinetics in deionized water at room temperature showed remarkable equilibrium swelling ratio values corresponding to 120, 186 and 200 for the hydrogels HG1, HG2 and HG3, respectively. Under different temperature and pH conditions the hydrogels showed a better swelling ratio at temperature 37 °C and pH 3 in comparison at 25 °C and pH 7.4. Cell viability studies showed that hydrogels have excellent antimicrobial activity. The release studies were carried out efficiently. The systems can retain and release neomycin sulfate in a controlled manner for 5 h. The HG1 hydrogel presented a lower release rate compared to the HG2 and HG3 hydrogels, releasing 71% of the drug at equilibrium. Estudied mathematical models reveal that the drug release mechanism was by chain relaxation. These results suggest that the hydrogels obtained may be potentially usable in the controlled release of neomycin sulfate.

References

1. Chiesa E, Genta I, Dorati R, Modena T, Conti B (2019) Poly(gamma-glutamic acid) based thermosetting hydrogels for injection: rheology and functional parameters evaluation. React Funct Polym 140:93–102. https://doi.org/10.1016/j.reactfunctpolym.2019.03.021
2. Ahmed EM (2015) Hydrogel: preparation, characterization, and applications: a review. J Adv Res 6(2):105–121. https://doi.org/10.1016/j.jare.2013.07.006
3. Ullah F, Othman MBH, Javed F, Ahmad Z, Akil HM (2015) Classification, processing and application of hydrogels: a review. Mater Sci Eng C 57:414–433
4. Hamedi H, Moradi S, Hudson SM, Tonelli AE (2018) Chitosan based hydrogels and their applications for drug delivery in wound dressings: a review. Carbohydr Polym 199(March):445–460. https://doi.org/10.1016/j.carbpol.2018.06.114
5. Peppas NA, Bures P, Leobandung W, Ichikawa H (2000) Hydrogels in pharmaceutical formulations. Eur J of Pharm Biopharm 50(1):27–46. https://doi.org/10.1016/S0939-6411(00)00090-4
6. Timur M, Paşa A (2018) Synthesis, characterization, swelling, and metal uptake studies of aryl cross-linked Chitosan hydrogels. ACS Omega 3(12):17416–17424. https://doi.org/10.1021/acsomega.8b01872
7. Peniche C, Argüelles-Monal W, Peniche H, Acosta N (2003) Chitosan: an attractive biocompatible polymer for microencapsulation. Macromol Biosci 3(10):511–520. https://doi.org/10.1002/mabi.200300019
8. Rinaudo M (2006) Chitin and chitosan: properties and applications. Prog Polym Sci (Oxford) 31(7):603–632. https://doi.org/10.1016/j.progpolymsci.2006.06.001
9. Dergunov SA, Mun GA (2009) γ-irradiated chitosan-polyvinyl pyrrolidone hydrogels as pH-sensitive protein delivery system. Radiat Phys Chem 78(1):65–68. https://doi.org/10.1016/j.radphyschem.2008.07.003
10. Moussout H, Ahlafi H, Aazza M, Bourakhouadar M (2016) Kinetics and mechanism of the thermal degradation of biopolymers chitin and chitosan using thermogravimetric analysis. Polym Degrad Stab 130:1–9. https://doi.org/10.1016/j.polymdegradstab.2016.05.016
11. Vunain E, Mishra AK, Mamba BB (2017) Fundamentals of chitosan for biomedical applications, vol 1. Elsevier. https://doi.org/10.1016/B978-0-08-100230-8.00001-7
12. Dimassi S, Tabary N, Chai F, Blanchemain N, Martel B (2018) Sulfonated and sulfated chitosan derivatives for biomedical applications: a review. Carbohydr Polym 202:382–396. https://doi.org/10.1016/j.carbpol.2018.09.011
13. Ahmed S, Ikram S (2016) Chitosan based scaffolds and their applications in wound healing. Achiev Life Sci 10(1):27–37. https://doi.org/10.1016/j.als.2016.04.001
14. Muxika A, Etxabide A, Uranga J, Guerrero P, de la Caba K (2017) Chitosan as a bioactive polymer: processing, properties and applications. Int J Biol Macromol 105:1358–1368. https://doi.org/10.1016/j.ijbiomac.2017.07.087
15. Mohammadzadeh Pakdel P, Peighambardoust SJ (2018) Review on recent progress in chitosan-based hydrogels for wastewater treatment application. Carbohydr Polym 201:264–279. https://doi.org/10.1016/j.carbpol.2018.08.070
16. Song Z, Li G, Guan F, Liu W (2018) Application of chitin/chitosan and their derivatives in the papermaking industry. Polymers. https://doi.org/10.3390/polym10040389
17. Wei H, Gao B, Ren J, Li A, Yang H (2018) Coagulation/flocculation in dewatering of sludge: a review. Water Res 143(2015):608–631. https://doi.org/10.1016/j.watres.2018.07.029
18. Ahmed S, Annu AA, Sheikh JA (2018) review on chitosan centred scaffolds and their applications in tissue engineering. Int J Biol Macromol 116(2017):849–862. https://doi.org/10.1016/j.ijbiomac.2018.04.176
19. Morin-Crini N, Lichtfouse E, Torri G, Crini G (2019) Fundamentals and applications of Chitosan, pp 49–123. https://doi.org/10.1007/978-3-030-16538-3_2
20. Habibie S, Hamzah M, Anggaravidya M, Kalembang E (2016) The effect of chitosan on physical and mechanical properties of paper. J Chem Eng Mater Sci 7(1):1–10. https://doi.org/10.5897/jcems2015.0235
21. Dash M, Chiellini F, Ottenbrite RM, Chiellini E (2011) Chitosan: a versatile semi-synthetic polymer in biomedical applications. Prog Polym Sci(Oxford) 36(8):981–1014. https://doi.org/10.1016/j.progpolymsci.2011.02.001

22. Bernkop-Schnürch A, Dünnhaupt S (2012) Chitosan-based drug delivery systems. Eur J Pharm Biopharm 81(3):463–469. https://doi.org/10.1016/j.ejpb.2012.04.007

23. Wei Z, Yang JH, Liu ZQ, Xu F, Zhou JX, Zrínyi M, Osada Y, Chen YM (2015) Novel biocompatible polysaccharide-based self-healing hydrogel. Adv Funct Mater 25(9):1352–1359. https://doi.org/10.1002/adfm.201401502

24. Ferreira MOG, Leite LLR, de Lima IS, Barreto HM, Nunes LCC, Ribeiro AB, Osajima JA, da Silva Filho EC (2016) Chitosan Hydrogel in combination with Nerolidol for healing wounds. Carbohydr Polym 152:409–418. https://doi.org/10.1016/j.carbpol.2016.07.037

25. Tsao CT, Chang CH, Lin YY, Wu MF, Wang JL, Han JL, Hsieh, KH (2010) Antibacterial activity and biocompatibility of a chitosan-γ- poly(glutamic acid) polyelectrolyte complex hydrogel. https://doi.org/10.1016/j.carres.2010.06.002

26. Lee YH, Chang JJ, Yang MC, Chien CT, Lai WF (2012) Acceleration of wound healing in diabetic rats by layered hydrogel dressing. Carbohydr Polym 88(3):809–819. https://doi.org/10.1016/j.carbpol.2011.12.045

27. Pereira CL, Antunes JC, Gonçalves RM, Ferreira-Da-Silva F, Barbosa MA (2012) Biosynthesis of highly pure poly-gamma-glutamic acid for biomedical applications. J Mater Sci Mater Med 23(7):1583–1591. https://doi.org/10.1007/s10856-012-4639-x

28. Puppi D, Migone C, Morelli A, Bartoli C, Gazzarri M, Pasini D, Chiellini F (2016) Microstructured chitosan/poly(γ-glutamic acid) polyelectrolyte complex hydrogels by computer-aided wet-spinning for biomedical three-dimensional scaffolds. J Bioact Comp Polym 31(5):531–549. https://doi.org/10.1177/0883911516631355

29. Yan X, Tong Z, Chen Y, Mo Y, Feng H, Li P, Qu X, Jin S (2017) Bioresponsive materials for drug delivery based on carboxymethyl chitosan/poly(gamma-glutamic acid) composite microparticles. Mar Drugs. https://doi.org/10.3390/md15050127

30. Torres J, Kremer C, Pardo H, Suescun L, Mombrú A, Castiglioni J, Domínguez S, Mederos A, Kremer E (2003) Preparation and crystal structure of new samarium complexes with glutamic acid. J Mol Struct 660(1–3):99–106. https://doi.org/10.1016/j.molstruc.2003.08.003

31. Fouad EA, El-Badry M, Alanazi FK, Arafah MM, Alsarra IA (2009) Preparation and investigation of acetyl salicylic acid-glutamic acid complex: a novel oral delivery system. Digest J Nanomater Biostruct 4(2):299–308

32. Singh J, Dutta PK, Dutta J, Hunt AJ, Macquarrie DJ, Clark JH (2009) Preparation and properties of highly soluble chitosan-l-glutamic acid aerogel derivative. Carbohydr Polym 76(2):188–195. https://doi.org/10.1016/j.carbpol.2008.10.011

33. Bregier-Jarzebowska R (2015) Mixed-ligand complexes of copper(II) ions with L-glutamic acid in the systems with triamines and non-covalent interaction between bioligands in aqueous solution. Open Chem 13(1):113–124. https://doi.org/10.1515/chem-2015-0038

34. Hemmati M, Kazemi B, Najafi F, Zarebkohan A, Shirkoohi R (2016) Synthesis and evaluation of a glutamic acid-modified hPAMAM complex as a promising versatile gene carrier. J Drug Target 24(5):408–421. https://doi.org/10.3109/1061186X.2015.1078338

35. Abdelwahab HE, Hassan SY, Mostafa MA, El Sadek MM (2016) Synthesis and characterization of glutamic-chitosan hydrogel for copper and nickel removal from wastewater. Molecules. https://doi.org/10.3390/molecules21060684

36. Thangavel P, Ramachandran B, Chakraborty S, Kannan R, Lonchin S, Muthuvijayan V (2017) Accelerated healing of diabetic wounds treated with l-glutamic acid loaded hydrogels through enhanced collagen deposition and angiogenesis: an in vivo study. Sci Rep 7(1):1–15. https://doi.org/10.1038/s41598-017-10882-1

37. Tsao CT, Chang CH, Li YD, Wu MF, Lin CP, Han JL, Chen SH, Hsieh KH (2011) Development of chitosan/ dicarboxylic acid hydrogels as wound dressing materials. J Bioact Comp Polym 26(5):519–536. https://doi.org/10.1177/0883911511422627

38. Shariatinia Z, Jalali AM (2018) Chitosan-based hydrogels: preparation, properties and applications. Int J Biol Macromol 115:194–220. https://doi.org/10.1016/j.ijbiomac.2018.04.034

39. Aycan D, Alemdar N (2018) Development of pH-responsive chitosan-based hydrogel modified with bone ash for controlled release of amoxicillin. Carbohydr Polym 184:401–407. https://doi.org/10.1016/j.carbpol.2017.12.023

40. Figueroa-Pizano MD, Vélaz I, Peñas FJ, Zavala-Rivera P, Rosas-Durazo AJ, Maldonado-Arce AD, Martínez-Barbosa ME (2018) Effect of freeze-thawing conditions for preparation of chitosan-poly (vinyl alcohol) hydrogels and drug release studies. Carbohydr Polym 195:476–485. https://doi.org/10.1016/j.carbpol.2018.05.004

41. Pinho E, Machado S, Soares G (2019) Smart hydrogel for the ph-selective drug delivery of antimicrobial compounds. Macromol Symp 385(1):1–7. https://doi.org/10.1002/masy.201800182
42. Lou C, Tian X, Deng H, Wang Y (2020) Jiang X (2020) Dialdehyde-β-cyclodextrin-crosslinked carboxymethyl chitosan hydrogel for drug release. Carbohydr Polym 231:115678. https://doi.org/10.1016/j.carbpol.2019.115678
43. Spann CT, Tutrone WD, Weinberg JM, Scheinfeld N, Ross B (2003) Topical antibacterial agents for wound care: a primer. Dermatol Surg 29(6):620–626. https://doi.org/10.1046/j.1524-4725.2003.29143.x
44. Nitanan T, Akkaramongkolporn P, Rojanarata T, Ngawhirunpat T, Opanasopit P (2013) Neomycin-loaded poly(styrene sulfonic acid-co-maleic acid) (PSSA-MA)/polyvinyl alcohol (PVA) ion exchange nanofibers for wound dressing materials. Int J Pharm 448(1):71–78. https://doi.org/10.1016/j.ijpharm.2013.03.011
45. Karadag E, Saraydin D (2002) Swelling of superabsorbent acrylamide/sodium acrylate hydrogels prepared using multifunctional crosslinkers. Turk J Chem 26(6):863–875
46. Korsmeyer RW, Gurny R, Doelker E, Buri P, Peppas NA (1983) Mechanisms of solute release from porous hydrophilic polymers. Int J Pharm 15(1):25–35. https://doi.org/10.1016/0378-5173(83)90064-9
47. Higuchi T (1961) Rate of release of medicaments from ointment bases containing drugs in suspension. Chem Pharm Bull. https://doi.org/10.1248/cpb.23.3288
48. Machín R, Isasi JR, Vélaz I (2013) Hydrogel matrices containing single and mixed natural cyclodextrins, Mechanisms of drug release. Eur Polym J 49(12):3912–3920. https://doi.org/10.1016/j.eurpolymj.2013.08.020
49. Costa P, Lobo JM (2001) Modeling and comparison of dissolution profiles. Pharm Sci 16(2):41–46. https://doi.org/10.14227/DT160209P41
50. Brugnerotto J, Lizardi J, Goycoolea FM, Argüelles-Monal W, Desbrières J, Rinaudo M (2001) An infrared investigation in relation with chitin and chitosan characterization. Polymer 42(8):3569–3580. https://doi.org/10.1016/S0032-3861(00)00713-8
51. Paulino AT, Simionato JI, Garcia JC, Nozaki J (2006) Characterization of chitosan and chitin produced from silkworm crysalides. Carbohydr Polym 64(1):98–103. https://doi.org/10.1016/j.carbpol.2005.10.032
52. Duarte ML, Ferreira MC, Marvão MR, Rocha J (2002) An optimised method to determine the degree of acetylation of chitin and chitosan by FTIR spectroscopy. Int J Biol Macromol 31(1–3):1–8. https://doi.org/10.1016/S0141-8130(02)00039-9
53. Valderruten NE, Valverde JD, Zuluaga F, Ruiz-Durántez E (2014) Synthesis and characterization of chitosan hydrogels cross-linked with dicarboxylic acids. React Funct Polym 84:21–28. https://doi.org/10.1016/j.reactfunctpolym.2014.08.006
54. Zou X, Zhao X, Ye L, Wang Q, Li H (2015) Preparation and drug release behavior of pH-responsive bovine serum albumin-loaded chitosan microspheres. J Ind Eng Chem 21:1389–1397. https://doi.org/10.1016/j.jiec.2014.06.012
55. Corazzari I, Nisticò R, Turci F, Faga MG, Franzoso F, Tabasso S, Magnacca G (2015) Advanced physico-chemical characterization of chitosan by means of TGA coupled on-line with FTIR and GCMS: thermal degradation and water adsorption capacity. Polym Degrad Stab 112:1–9. https://doi.org/10.1016/j.polymdegradstab.2014.12.006
56. Martínez-Camacho AP, Cortez-Rocha MO, Ezquerra-Brauer JM, Graciano-Verdugo AZ, Rodriguez-Félix F, Castillo-Ortega MM, Yépiz-Gómez MS, Plascencia-Jatomea M (2010) Chitosan composite films: thermal, structural, mechanical and antifungal properties. Carbohydr Polym 82(2):305–315. https://doi.org/10.1016/j.carbpol.2010.04.069
57. Prakash G, Boopathy M, Selvam R, Johnsanthosh Kumar S, Subramanian K (2018) The effect of anthracene-based chalcone derivatives in the resazurin dye reduction assay mechanisms for the investigation of Gram-positive and Gram-negative bacterial and fungal infection. New J Chem 42(2):1037–1045. https://doi.org/10.1039/C7NJ04125J
58. Severino R, Vu KD, Donsì F, Salmieri S, Ferrari G, Lacroix M (2014) Antibacterial and physical effects of modified chitosan based-coating containing nanoemulsion of mandarin essential oil and three non-thermal treatments against Listeria innocua in green beans. Int J Food Microbiol 191:82–88. https://doi.org/10.1016/j.ijfoodmicro.2014.09.007
59. Goy RC, De Britto D, Assis OBG (2009) A review of the antimicrobial activity of chitosan. Polimeros 19(3):241–247. https://doi.org/10.1590/S0104-14282009000300013

60. Goy RC, Morais STB, Assis OBG (2016) Evaluation of the antimicrobial activity of chitosan and its quaternized derivative on E. Coli and S. aureus growth. Braz J Pharmacogn 26(1):122–127. https://doi.org/10.1016/j.bjp.2015.09.010

61. Zhang Y, Huo M, Zhou J, Zou A, Li W, Yao C, Xie S (2010) DDSolver: an add-in program for modeling and comparison of drug dissolution profiles. AAPS J 12(3):263–271. https://doi.org/10.1208/s12248-010-9185-1

Publisher's Note Springer Nature remains neutral with regard to jurisdictional claims in published maps and institutional affiliations.